The Journal of Experimental Biology 201, 731–744 (1998)
Printed in Great Britain © The Company of Biologists Limited 1998
JEB1195

FOREWING MOVEMENTS AND INTRACELLULAR MOTONEURONE STIMULATION IN TETHERED FLYING LOCUSTS

B. HEDWIG* AND G. BECHER

I. Zoologisches Institut, Berliner Straße 28, D-37073 Göttingen, Germany

*Present address: Department of Zoology, Downing Street, Cambridge CB2 3EJ, UK (e-mail: bh202@cam.ac.uk)

Accepted 8 December 1997: published on WWW 5 February 1998

Summary

A new optoelectronic method was used for the measurement of wing movements in tethered flying locusts. The method is based on laser light coupled into a highly flexible optical fibre fastened to a forewing. A dual-axis position-sensing photodiode, aligned to the wing hinge, revealed the flapping, i.e. up–down movement, and lagging, i.e. forward–backward movement, of the wingtip as indicated by the emitted light. Measurements were combined with electromyographic recordings from flight muscles and with intracellular recording and stimulation of flight motoneurones. Compared with muscle recordings, intracellular recordings showed an increase in the variability of motoneurone activity. Stimulation of flight motoneurones reliably caused distinct effects on wing movements. Inhibition of elevator (MN83, MN89) activity led to a decrease in the amplitude of the upstroke. Inhibition of depressor (MN97) activity reduced the amplitude of the downstroke and sometimes stopped flight behaviour. An increase in MN97 activity caused a reduction in the extent of the upward movement and prolonged the flight cycle.

Key words: insect, locust, *Locusta migratoria*, flight, optoelectronic measurement, wing movement, motoneurone activity.

Introduction

In the analysis of locust flight, two major areas of interest are the biophysics of flight behaviour and its neurophysiological control mechanisms.

High-speed motion-picture cameras (Weis-Fogh and Jensen, 1956; Baker, 1979; Robertson and Reye, 1992) and stereophotogrammetry (Zarnack, 1972) have been used in the study of wing kinematics. These methods, however, can be used for the analysis of short flight sequences only. Therefore, the development of an inductive method for the continuous measurement of wing movements represented a major advance in this field (Koch, 1977; Zarnack, 1978). This method quantifies the different components of wing movement: flapping (up–down), lagging (forward–backward) and pitching (pronation–supination) and can be applied to all four wings simultaneously (Schwenne and Zarnack, 1987). It can also be combined with electromyographic recordings from flight muscles (Zarnack, 1988; Waldmann and Zarnack, 1988; Reuse, 1991) and with measurements of the flight forces produced by the animal (Wortmann, 1991). However, only extracellular recording techniques can be used since the devices necessary for intracellular recordings cause distortions of the electromagnetic measuring conditions.

Neurophysiological investigations of locust flight behaviour have been aimed at understanding the interactions among the central nervous system, the sense organs and the effectors that underlie flight activity. The development of a locust flight preparation that allowed intracellular recordings from moto- and interneurones in minimally dissected tethered flying locusts (Wolf and Pearson, 1987*a*) represented a major advance. Using this preparation, electromyographic recordings from flight muscles were used to monitor flight activity. In this way, the special role of sensory feedback in the generation of the flight motor pattern has been demonstrated (Wolf and Pearson, 1988).

Combinations of the neurophysiological and the biophysical approaches to locust flight behaviour may lead to a better understanding of the interactions among motor activity, wing movements and flight behaviour. Simultaneous intracellular recordings and optoelectronic monitoring of the flapping movement have been used previously by Wolf (1993) to analyse tegula function. The present study describes a new optoelectronic method for the two-dimensional recording of wing movements (Hedwig and Becher, 1995) which can be combined with intracellular recordings and stimulation of flight neurones to provide a new comprehensive analysis of locust flight behaviour.

Materials and methods

Animals

Adult locusts (*Locusta migratoria* L.) were taken from a crowded colony kept in the Zoological Department, University

of Göttingen, Germany. Male and female animals were used 2–4 weeks after the final moult. The locusts selected had forewings 50 mm in length and were ready to fly. All experiments were performed at 26–28 °C.

Preparation

The preparation of the locusts was carried out as described by Wolf and Pearson (1987*a*). In brief, animals were fixed upside down in a holder and the hind, front and middle legs were fixed in the flight position. The cuticle above the mesothoracic ganglion was opened. A small ring of wax was placed around the opening in the cuticle, and the exposed ganglion was covered with a drop of saline (Usherwood and Grundfest, 1965). For intracellular recordings, the ganglion was mechanically stabilized using modified coverslip forceps. The lower part of the forceps was designed as a platform and the upper part as a ring. The forceps were positioned using a micromanipulator such that the ganglion was situated between the platform and the ring. Intracellular recordings were obtained within the ring.

Locusts (N=140) were flown under open-loop conditions. Flight sequences were elicited by blowing wind onto the head of the animals. The eyes were covered with black paint. The effects of motoneurone stimulation were confirmed in at least three separate experiments.

Electromyographic recordings

Muscle recordings from an elevator (M83, tergosternal) and a depressor (M97, first basalar) muscle were made ipsilateral to the wing movement recordings. For this purpose, two stainless-steel wires 30 μm in diameter were inserted into the sternal attachment sites of the muscles (Wolf and Pearson, 1988).

Intracellular recordings

Microelectrodes were pulled (David Kopf vertical pipette puller 700C) from borosilicate glass capillaries (o.d. 1.0 mm, i.d. 0.5 mm, Hilgenberg). The tip of the electrodes was filled with Lucifer Yellow (5 % in distilled water), and the shaft of the electrodes was filled with LiCl (1 % in distilled water). Electrodes had a resistance of 80–120 MΩ and were positioned using a micromanipulator (Leitz). The platform used for mechanical stabilization of the ganglion (see above) was used as a reference electrode. Recordings from motoneurones were made in the main dendritic branches in the neuropile and were amplified using a d.c. amplifier (List L/M-1). Current injection for motoneurone stimulation was performed in the bridge mode. Voltage pulses of approximately 350 ms duration of either polarity were generated using a pulse generator with a stimulus isolation unit (WPI anapulse stimulator with 302-T unit).

Intracellular staining of the motoneurones were carried out using Lucifer Yellow (Stewart, 1978) for identification of the motoneurones. Standard procedures were followed for staining and histology.

Measurement of forewing movements

Flapping and lagging movements of a forewing were measured using an optoelectronic method (Fig. 1). One end of a highly flexible plastic optical fibre 500 mm in length (Mitsubishi Rayon Co., type CK-4, 93 μm diameter, mass 1 mg per 10 mm, numerical aperture 0.47) was glued (Marabu rubber glue) to the dorsal surface of the left forewing. The optical fibre followed the radial vein and ended at the wingtip (Fig. 1A). The other end of the fibre was heat-polished. It was positioned in a multimode optical-fibre coupler (Newport, F-916T) in the focal plane of a 10× microscope objective (Newport M-10X, numerical aperture 0.25). The light of a d.c. 10 mW He–Ne laser (Melles Griot, 05 LHP 991) was coupled to the optical fibre with an efficiency of at least 70 %. At the wingtip, the laser light emitted from the end of the fibre formed a bright spot (Fig. 1A). The spot indicated the movements of the wingtip during flight. Photographs of the wingtip path of a complete wingbeat cycle could be taken using a camera with the shutter set to 1/15 s (Fig. 1B).

The position and the movement of the wingtip as indicated by the laser light were measured using a highly linear dual-axis position-sensing photodiode (United Detector Technology, PIN DLS-20). The diode had an active area of 20 mm×20 mm and was fitted to a camera in the same plane as the film. The camera (lens aperture 1.4, f=50 mm) was positioned at a distance of 500 mm from the wingtip, and the photodiode was precisely centred on the wing base. At this distance, the measurement field covered by the diode was 125 mm×125 mm. The electronic circuit delivered two analogue output voltages, an x- and y-signal that indicated the lagging (x-coordinate) and the flapping (y-coordinate) movements of the wing, respectively. These measurement correspond to a projection of the wingtip movement onto a plane; whereas the angular deviation of the wing is the arcsine function of this projection. (The relationship between both measures is exemplified in Fig. 3C. Data in the text refer to the two-dimensional projection of the movement.)

The working range of the optoelectronic system was checked in several experiments.

Intensity function of the diode

Position-sensing photodiodes deliver output signals which are proportional to the position and, at the limits of sensitivity, to the intensity of the spot of light. To test the intensity function of the complete optoelectronic circuit, the tip of the light guide was positioned 50 mm lateral to the centre of the diode (see Fig. 2C) at a distance of 500 mm from the camera, as under normal measuring conditions. The light intensity measured directly in front of the camera (Gossen luxmeter, type Mavolux) was gradually decreased in steps of 0.05 lx, and the output voltage of the electronic circuit was determined simultaneously (Fig. 2A). At intensities between 0.25 and 0.5 lx, the output signal of the diode indicating the position of the optical fibre was constant. At lower intensities, however, an increasing error occurred; at 0.1 lx, the error was 10 %. Thus, for precise measurements, the camera had to receive light intensities in the range 0.25–0.5 lx.

Angular emission function of the optical fibre

The CK-4 optical fibre has a numerical aperture of 0.47. Therefore most of the light is emitted/accepted between –28 and

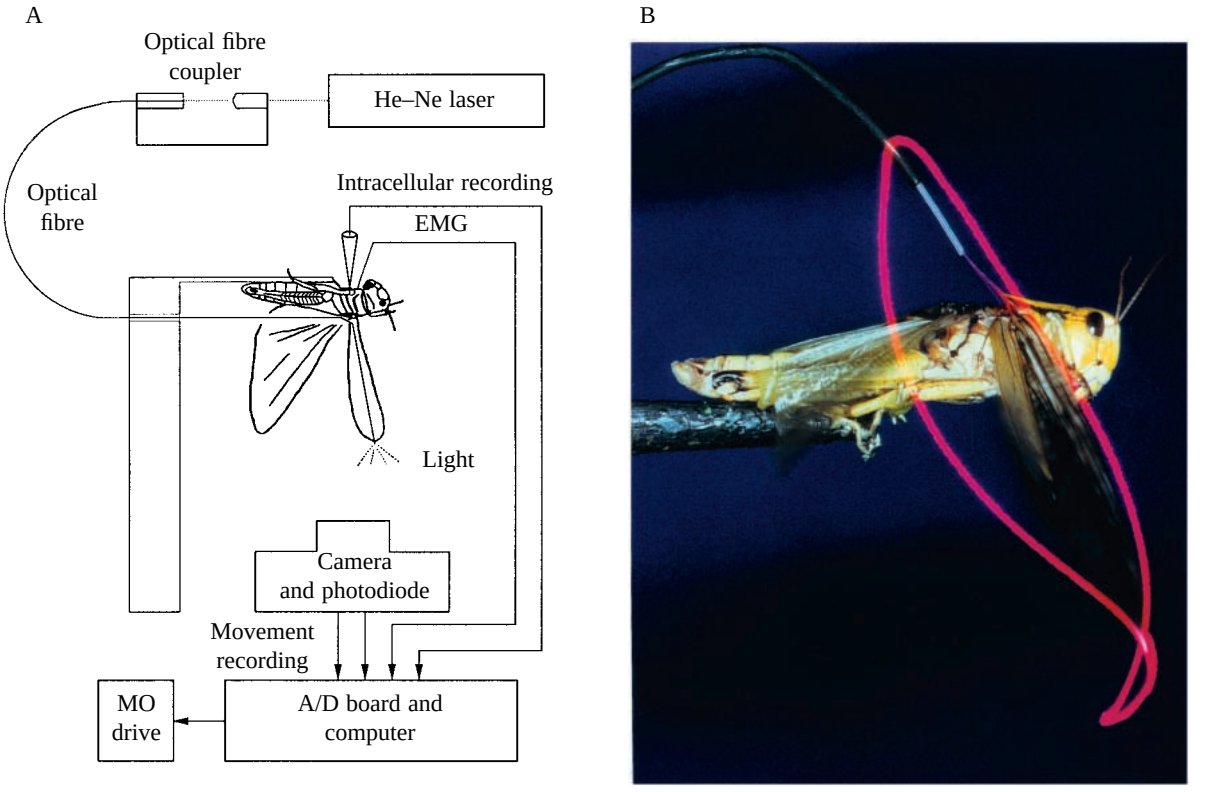

Fig. 1. (A) Experimental arrangement for simultaneous measurement of wing movements, intracellular recordings from flight motoneurones and electromyographic recordings from flight muscles. The locusts were flown upside down. Data were sampled on-line and stored on a magneto-optical disk drive (MO). For further details, see text. (B) Photograph (1/15 s exposure) of a tethered flying locust with a CK-4 optical fibre attached and emitting a laser light (red) at its tip. This animal was in the normal flight position and was not prepared for intracellular recordings.

+28 °. The angular emission function of the fibre was investigated by moving its tip in steps of 5 ° while measuring the light intensity at a distance of 500 mm (Fig. 2B). At 0 °, the maximum light intensity reaching the camera was 5.4 lx. However, by 70 ° the intensity had decreased to 0.005 lx. Since the locust wing might reach an angle of 70 ° at either end of a stroke, this emission function means that there would not be enough light present for precise measurements to be obtained (see intensity function of diode, Fig. 2A). To produce a broader emission from the optical fibre, the emission function was altered by covering the end of the fibre with a layer of titanium (IV) dioxide (TiO_2, Sigma) mixed with histological embedding medium, scattering the

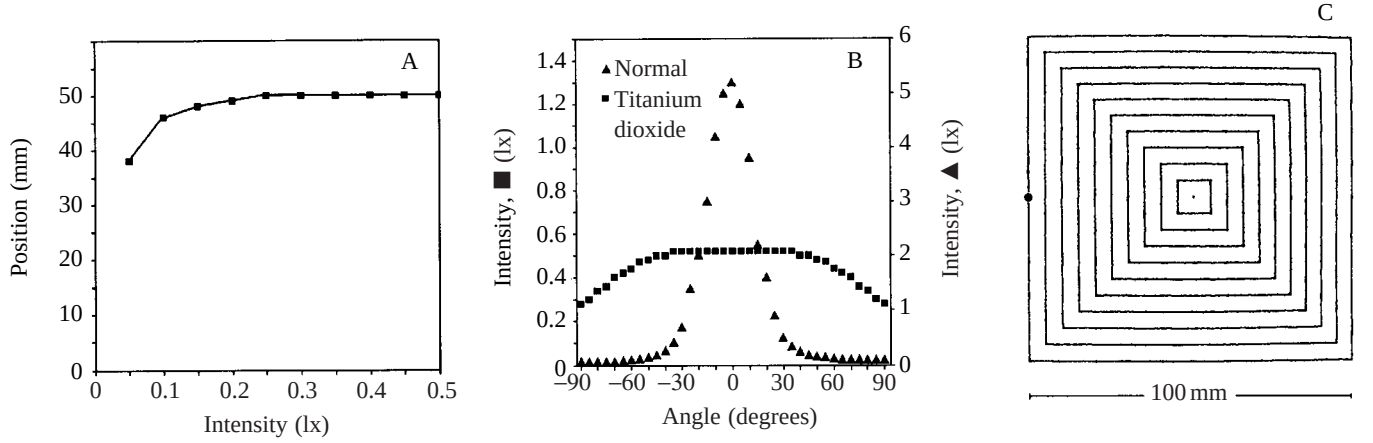

Fig. 2. (A) Intensity function of the photodiode and electronic circuit. The optical fibre was held stationary in the measurement plane at x=−50 mm and y=0 mm (position indicated by a black circle in C). The light intensity emitted from the fibre tip was gradually decreased. The system gave a constant output at intensities greater than 0.25 lx. (B) Angular emission function of the optical fibre before (triangles, right ordinate) and after (squares, left ordinate) covering the tip with titanium dioxide. (C) Reproduction by the optoelectronic system of concentric squares produced by the movement of a plotter head to which the optical fibre was attached.

emitted light. This resulted in a broad, flat emission function with a minimum light intensity of 0.35 lx at 70° and 0.28 lx at 90° (Fig. 2B). This emission function was within the linear range of the intensity function (see Fig. 2A). The layer of titanium dioxide also had a positive effect on the speckled pattern of the emitted light; it reduced both the size of the speckles and the contrast between them, thus improving the optical signal.

Accuracy of depiction

The spatial accuracy of the system was tested using a plotter to which the optical fibre was attached oriented towards the photodiode. A software program was used to make the plotter produce concentric squares of increasing size. The largest square had sides 100 mm long. The camera was positioned at a distance of 500 mm from the plotter and was aligned with the centre of the squares. The optoelectronic measuring system reproduced the squares with high precision (Fig. 2C). Since locusts used in experiments had a wing length of 50 mm, the complete movement path of the wingtip was within the linear measuring range of the diode.

Temperature effects

The DLS 20 photodiode is very sensitive to changes in temperature. Room temperature fluctuations of ±1–2 °C produce significant changes in the diode's current. The diode was therefore mounted on a Peltier element and its temperature was kept constant at 22 °C.

Data sampling and evaluation

All recordings were sampled on-line at 10 kHz per channel. For this purpose, an A/D board (Data Translation, DT 2821 F8DI), the software Turbolab (Bressner Technology, Gröbenzell) and an IBM-compatible personal computer were used. Data files were stored on a magneto-optical disk system (Sony SMO 521). Data evaluation was carried out using the software package NEUROLAB (Hedwig and Knepper, 1992; Knepper and Hedwig, 1996). This software contains comprehensive functions allowing the display, analysis and plotting of neurobiological data. Phase-dependent averaging of the movement components was carried out as follows. All cycles of the flapping movement

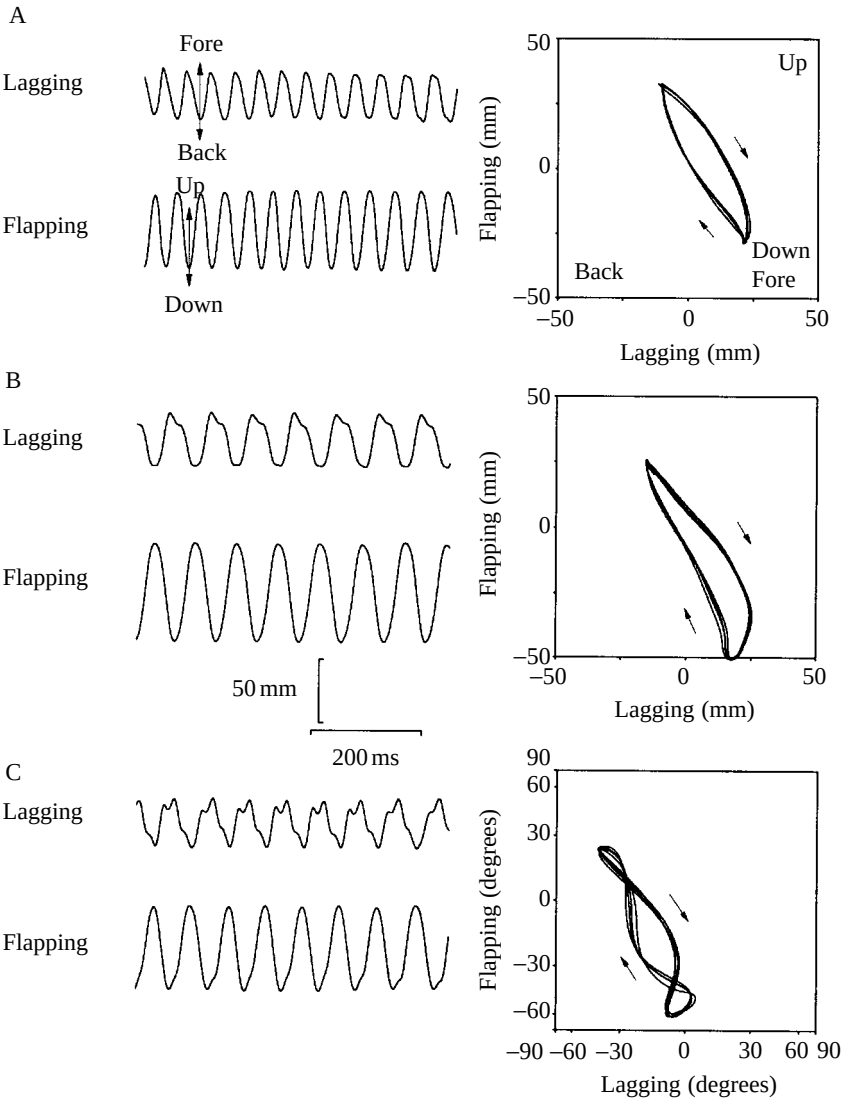

Fig. 3. Three examples of patterns of wingtip movements obtained in different flight sequences. The time functions (left) and the resulting two-dimensional projections of the wingtip path (right) are shown. Arrows indicate the direction of wing movement. The axes in C are in degrees and give the angle of the wing relative to the camera. Note the nonlinear scaling.

were standardized to a unit length of 1. The time functions of the flapping and lagging movements were then averaged with respect to the standardized flapping cycles. All frequency distributions were divided by the number of cycles evaluated to allow comparisons among different histograms.

Results

Wing movements of intact locusts

Flight was initiated by blowing wind towards the head of the locusts; once flight had been established, no further wind stimulus was given. The animals were flown under open-loop conditions, so their flight activity had no visual or aerodynamic feedback effects. Flight sequences of up to 15 min were obtained. Wingbeat frequency varied between 14 and 22 Hz. In general, it was high at the beginning of a flight sequence and then decreased gradually. In a first set of experiments, we measured the movement patterns of the forewing without additional electrophysiological recordings.

The movement pattern of the wing was not identical in different flight sequences (Fig. 3). Lagging movements were approximately 45° in amplitude peak-to-peak, whereas flapping movements reached 120° in amplitude peak-to-peak. Flapping movements had a regular sinusoidal appearance and were similar among different animals, whereas lagging movements showed some degree of variability. At the anterior or posterior end of a stroke, the lagging movement sometimes had a step-like form (Fig. 3B,C). Since the flapping and lagging movements were measured simultaneously, the two-dimensional path of the wingtip could be reconstructed. Generally, the wingtip path had an approximately oval shape in stable flight sequences (Fig. 3A). However, where the lagging movement contained step-like changes, the oval was sometimes narrower or had one or two crossovers (Fig. 3B,C). Thus, different movement paths of the wingtip were correlated with changes in the lagging movement.

Muscle activity and wing movements

Electromyographic recordings from an ipsilateral elevator (M83) and depressor (M97) muscle were made to analyse the timing and spatial correspondence between muscle activity and the wingtip path. The muscles showed an activity of 2–3 potentials per cycle at the beginning of a flight sequence, decreasing to approximately 1 potential per cycle during the

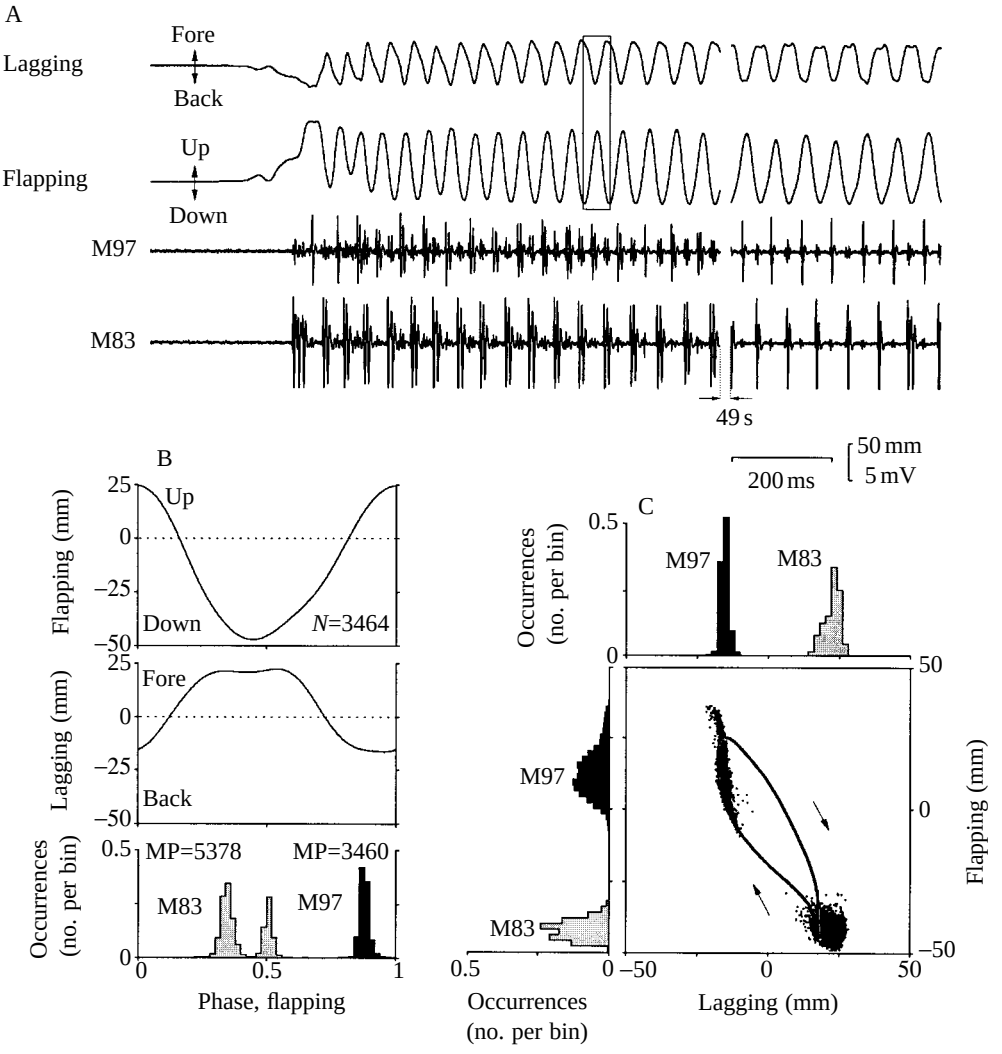

Fig. 4. Relationship between flight muscle activity and wing movements. (A) Simultaneous recording of two wingtip movement components and elevator (M83) and depressor (M97) muscle activity at the beginning and in the middle of a flight sequence. Minor potentials in the electromyograms are due to cross-talk. (B) Phase-dependent averages of the flapping movement and the lagging movement and a phase histogram of the muscle activity (bin width 0.02). (C) Scatter diagram representing the wingtip position at the moment of muscle activity for one complete flight sequence. Data corresponding to elevator (M83) activity form a dense cluster at the end of the downstroke; those for depressor (M97) activity form an elongated band at the end of the upstroke. The wingtip path from a single cycle (indicated by a box in A) is also shown (arrows indicate the direction of wing movement). Amplitude histograms of the lagging movement (top) and the flapping movement (left) at the moment of muscle activity are also presented. Black histograms correspond to M97 activity and shaded histograms correspond to M83 activity. MP, number of muscle potentials analysed.

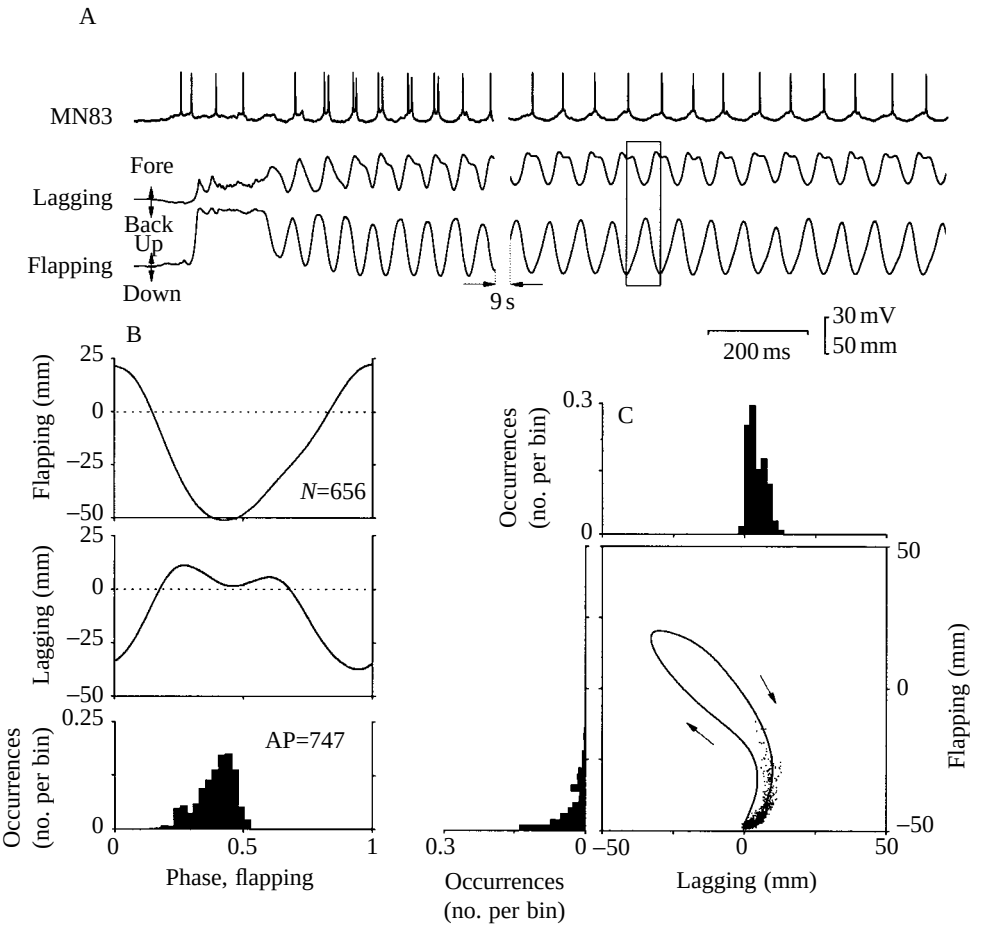

Fig. 5. (A) Intracellular recording from the elevator motoneurone MN83 with simultaneously recorded components of wingtip movement at the beginning and in the middle of a flight sequence. (B) Phase-dependent averages of the flapping movement and the lagging movement and a phase histogram of the motoneurone spike activity (bin width 0.02). (C) Scatter diagram representing the wingtip position at the moment of motoneurone activity. The movement path of a single flight cycle (indicated in A) is also shown (arrows indicate the direction of wing movement). Amplitude histograms are for the lagging movement (top) and the flapping movement (left) at the moment of motoneurone spike activity. AP, number of action potentials analysed.

sequence (Fig. 4A). The phase relationship between flapping and lagging movements was calculated by phase-dependent averaging of both components (see Materials and methods). Phase histograms of muscle activity were calculated with respect to the end of the upstroke (Fig. 4B).

In Fig. 4A, the sinusoidal flapping movement of the wing is clear. The averaged phase diagram of the flapping movement (Fig. 4B) shows that the end of the downstroke occurs at phase 0.45, indicating that the downward movement was slightly faster than the upward movement. With respect to the flapping movement, the lagging movement reached its most anterior position before the end of the downstroke, remaining at this value until the wing had begun to move upwards again. Similarly, the most posterior position of the wing is reached before the end of the upstroke and the wing remains in this position until the beginning of the downstroke (Fig. 4B). The phase histograms of muscle activity (Fig. 4B) demonstrate that elevator (M83) activity started at phase 0.3, just before the wing reached its lowest and most anterior position. A second period of elevator activity occurred at phase 0.5, i.e. at the beginning of the upstroke. The depressor M97 was active at phase 0.9, just before the end of the upstroke when the wing reached its most retracted position.

For every muscle potential, the *x*- and *y*-coordinates of the wingtip position were also determined, allowing the spatial relationship between muscle activity and wingtip position to be determined. Fig. 4C shows the frequency distribution of the movement amplitudes corresponding to muscle activity. For the flapping movement, maximum M83 activity occurred at $y=-45$ mm; the movement amplitude histogram for M97 activity was broader, with a maximum at approximately $y=10$ mm. For the lagging movement, the peaks of muscle activity were at $x=24$ mm (M83) and at $x=-16$ mm (M97).

These data were plotted on a scatter diagram showing the position of the wingtip at the corresponding period of muscle activity (Fig. 4C). To illustrate further the relationship between muscle activity and wing movement, the wingtip path of a single flight cycle is superimposed on Fig. 4C (note that the plotted points correspond to complete flight sequences not to single cycles). The wing positions corresponding to elevator activity form a dense cluster at the end of the downstroke, while the positions at which the depressor was active form a narrow band in the second half of the upstroke. Thus, from these muscle recordings, the wing positions corresponding to both M83 elevator and M97 depressor activity had characteristic spatial distributions with very little scatter.

Intracellular recording of motoneurone activity and wing movements

The activity of elevator motoneurones (MN83, MN89,

MN90) and of direct depressor motoneurones (MN97, MN98) was recorded together with electromyograms from flight muscles and forewing movements. As examples, intracellular recordings from the elevator MN83 and depressor MN97 are discussed below.

Elevator motoneurone MN83

Elevator motoneurone MN83 (anterior tergosternal) was depolarized by the wind stimulus and began spiking before the wing began to move upwards (Fig. 5A). Thereafter, the membrane potential oscillated in the flight rhythm and the motoneurone was active with 1–2 spikes per movement cycle. The phase histogram (Fig. 5B) shows that spike activity occurred between phase 0.25 and 0.5, corresponding to the second half of the downstroke. The peak of activity was at phase 0.45, just before the end of the downstroke (Fig. 5B).

The wing positions corresponding to MN83 activity are shown in the amplitude histograms and in the scatter diagram in Fig. 5C. The amplitude histogram for the flapping movement reveals an asymmetrical frequency distribution. It indicates that, when the action potentials of the elevator occurred, the wingtip was in a position between y=−25 mm and y=−50 mm (Fig. 5C). The amplitude histogram for the lagging movement when MN83 was active shows a clear maximum at x=3 mm (Fig. 5C, top). The scatter diagram also demonstrates that there was increased scatter in the wing positions corresponding to elevator activity during these intracellular recordings compared with experiments in which only EMG recordings were made (see Fig. 4). Elevator activity began during the second half of the downstroke, with the main period of activity occurring just before the upstroke began.

Depressor motoneurone MN97

Depressor motoneurone MN97 (first basalar) received small inhibitory postsynaptic potentials during the wind stimulus. It exhibited rhythmic membrane potential oscillations during the flight sequences (Fig. 6A). Within a flight cycle, the motoneurone was depolarized at the beginning of the upstroke, and depolarization was maximal just before the upper reversal point of the wing. The motoneurone usually generated two action potentials and then rapidly repolarized (Fig. 6A).

The phase histogram (Fig. 6B) shows that the first spike of MN97 occurred at phase 0.74 and the second at 0.88 within the upstroke. With respect to the lagging movement, the spikes occurred as the wing approached its most backward position (Fig. 6B).

The wing positions corresponding to MN97 spikes had a rather broad distribution and occurred during the upstroke between y=0 and y=40 mm (Fig. 6C). With respect to the lagging movement, most of the spikes occurred when the wing

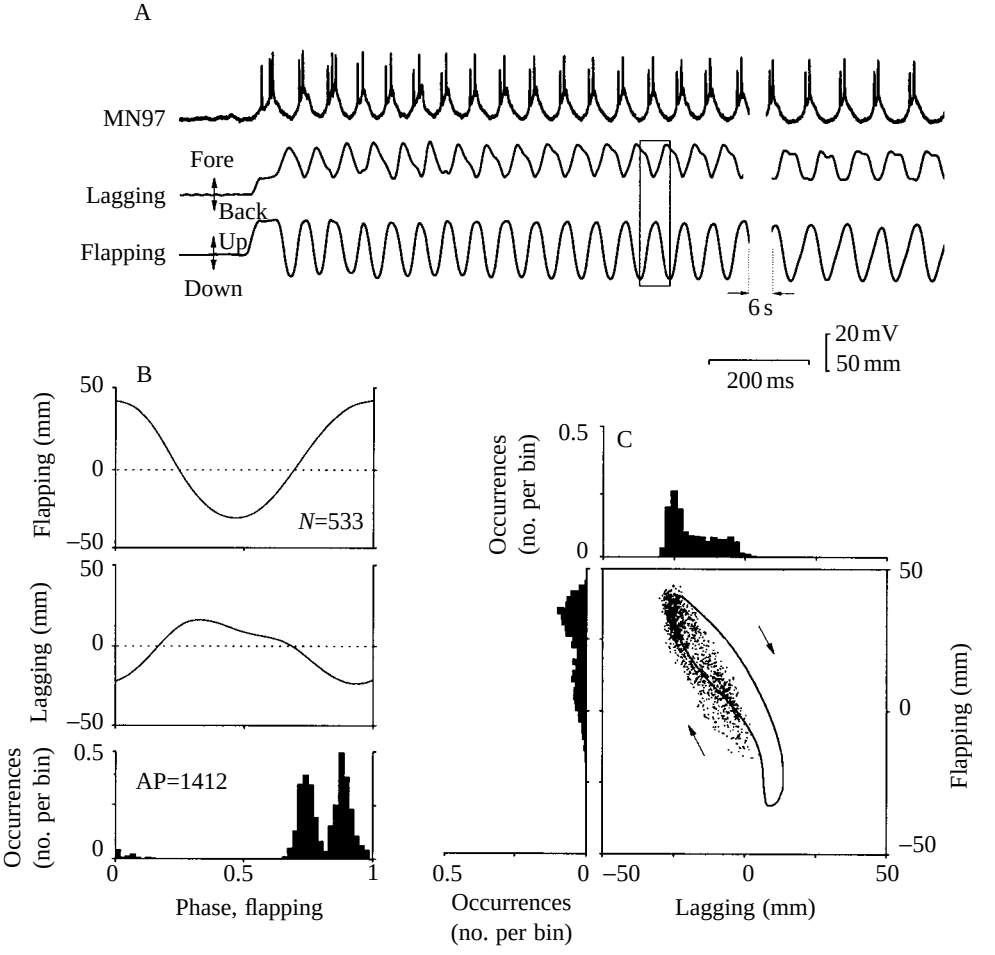

Fig. 6. (A) Activity of depressor motoneurone MN97 and simultaneously recorded components of the wing movement at the beginning and in the middle of a flight sequence. (B) Phase-dependent averages of the flapping movement and the lagging movement and a phase histogram of the motoneurone spike activity. (C) Scatter diagram representing the wingtip position at the moment of motoneurone activity. The wingtip positions corresponding to motoneurone activity form a broad elongated cluster during the upstroke. The movement path of a single flight cycle (indicated in A) is also shown (arrows indicate the direction of wing movements). Amplitude histogram are for the lagging movement (top) and the flapping movement (left) at the moment of motoneurone activity. AP, number of action potentials analysed.

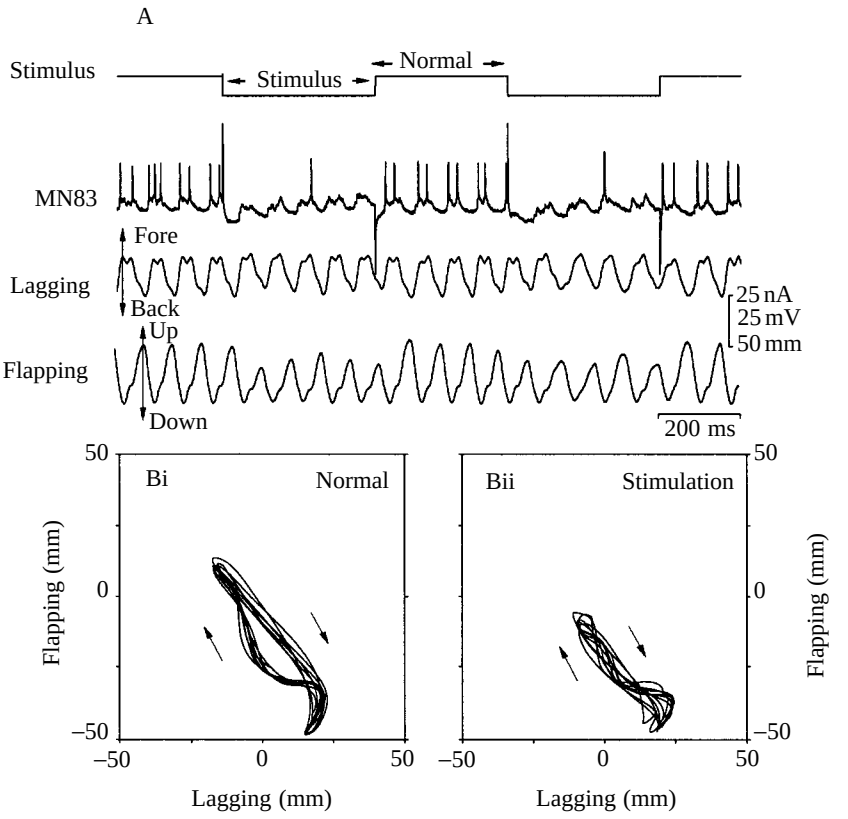

Fig. 7. (A) Effects of stimulation of elevator motoneurone MN83 on wing movements. Hyperpolarizing current injection into the motoneurone resulted in an almost complete suppression of its spike activity and a decrease in the amplitude of the upward movement of the wing. (B) Wingtip path during normal flight cycles (Bi, left) and during flight cycles with MN83 inhibition (Bii, right). Five wingtip paths were superimposed. The arrows indicate the direction of wing movement.

was at a position between x=0 mm and x=–27 mm, with a maximum at x=–25 mm (Fig. 6C). The first spike of MN97 within a movement cycle occurred in the middle of the upstroke, with the second spike occurring before the upper reversal point of the wing. As a consequence, in the scatter diagram of Fig. 6C, the wing positions corresponding to MN97 action potentials form a rather broad elongated band within the upstroke (compare with Fig. 4).

Intracellular stimulation of motoneurones during flight sequences

A causal analysis of the relationship between motoneurone activity and wing movements was carried out by experimental modulation of neuronal activity. We used intracellular current injection (350 ms duration, 700 ms interval) and altered the spike activity of single motoneurones during simultaneous recordings of wing movements. Elevator motoneurones MN83, MN89 and MN90 and depressor motoneurones MN97 and MN98 were stimulated.

Stimulation of motoneurone MN83

Tergosternal muscle M83 is one of the largest muscles in the mesothoracic segment. Motoneurone MN83 generally exhibited two and occasionally three action potentials per wingbeat cycle. Enhancing the number of spikes per wingbeat cycle from two to three spikes per burst did not affect the wing movement. However, injection of inhibitory current, which decreased motoneurone activity, did alter the pattern of wing movement (Fig. 7A,B).

In normal flight sequences, the lower reversal point of the wingtip was at y=–48 mm and the upper reversal point was at y=15 mm (Fig. 7B). During inhibitory current injection, spike activity was either suppressed completely or reduced to a single spike per wingbeat cycle. Correlated with this reduction in motoneurone activity were clear changes in wingtip movement. The position of the lower reversal point remained unchanged; however, the upstroke amplitude clearly decreased. The upper reversal point of the wing was at approximately y=–12 mm, representing a 27 mm reduction. The wing also did not move as far backwards as during normal flight, and the position of the upper reversal point shifted from x=–17 mm to x=–11 mm.

In some cases, suppression of spike activity was incomplete, and a single spike was generated during a wingbeat cycle. In these cases, the amplitude of the upstroke was greater than during complete inhibition, although still smaller than during movement cycles in which two MN83 action potentials occurred (Fig. 7A). Thereafter, the position of the upper reversal point of the wing movement depended on the number of spikes in MN83. We did not observe an effect on the lower reversal point, which remained constant (Fig. 7B).

Stimulation of motoneurone MN89

The anterior tergocoxal muscle M89 is smaller in size than the tergosternal muscle M83 and consists of two motor units. During flight sequences, motoneurone MN89 generated 2–3 action potentials (Fig. 8A). The upper reversal point of the wingtip occurred at y=26 mm and the lower reversal point was

at y=–48 mm. The total movement amplitude was 74 mm (Fig. 8B). With inhibitory current pulses of –6 nA, the number of spikes in the motoneurone could be reduced transiently to one spike per wingbeat cycle. This decrease in activity resulted in clear changes in the wing movement (Fig. 8A,B). The position of the upper reversal point was reduced to approximately y=12 mm and also occurred at a more anterior position. The peak-to-peak amplitude of the wing movement was reduced to approximately 60 mm. Thus, the activity of a single motor unit of elevator motoneurone MN89 can modify the amplitude of the upward movement and therefore the position of the upper reversal point. Stimulation of motoneurone MN89 did not alter the position of the lower reversal point (Fig. 8).

Elevator motoneurone MN90 (posterior tergocoxal) was also tested during flight sequences. In this case, we were able either to increase the number of spikes per cycle from two to four or to suppress the activity of the motoneurone completely. However, in neither case were obvious changes in wing movements observed (data not presented).

Stimulation of depressor motoneurone MN97

The first basalar muscle is a depressor innervated by one motoneurone (MN97). MN97 was stimulated with hyperpolarizing and depolarizing current pulses (7 nA for 350 ms) during flight sequences. During normal flight, the motoneurone generated three spikes per wingbeat cycle (Figs 9A, 10A) which occurred in the second half of the wing upstroke just before the upper reversal point. The upstroke and the downstroke of the wing were very regular, with a total movement amplitude of approximately 66 mm. The lagging movement had a more triangular waveform, with the anterior position of the wing at approximately x=15 mm and the posterior position at approximately x=–27 mm (Figs 9B, 10B). The two-dimensional projection of the wing movement had an elongated oval shape.

Inhibition of motoneurone MN97 during flight sequences either decreased its spike activity or abolished it completely (Fig. 9A). Reducing spike activity from three action potentials per cycle to one action potential per cycle caused only minor changes in the wing movement, which was shifted slightly upwards without any change in movement amplitude. Complete inhibition of MN97 spike activity, however, caused dramatic changes in wing movement (Fig. 9A). Immediately following the failure of MN97 activity, the downstroke of the wing was reduced to approximately half of its normal amplitude. The wing was then lifted again and remained in this lifted and retracted position (Fig. 9Bii). The wing performed rudimentary oscillations only, and flight behaviour ceased.

Depolarizing current injection increased the number of spikes from three to four or even five action potentials per cycle (Fig. 10A). This resulted in a phase shift of activity, with depressor activity occurring earlier in the wingbeat cycle. The first spike of the burst occurred before the lower reversal point of the wing at the beginning of the upward movement (Fig. 10A). As a consequence of this altered motoneurone activity, there were dramatic changes in the wing movement. The earlier and increased depressor activity led to a significant

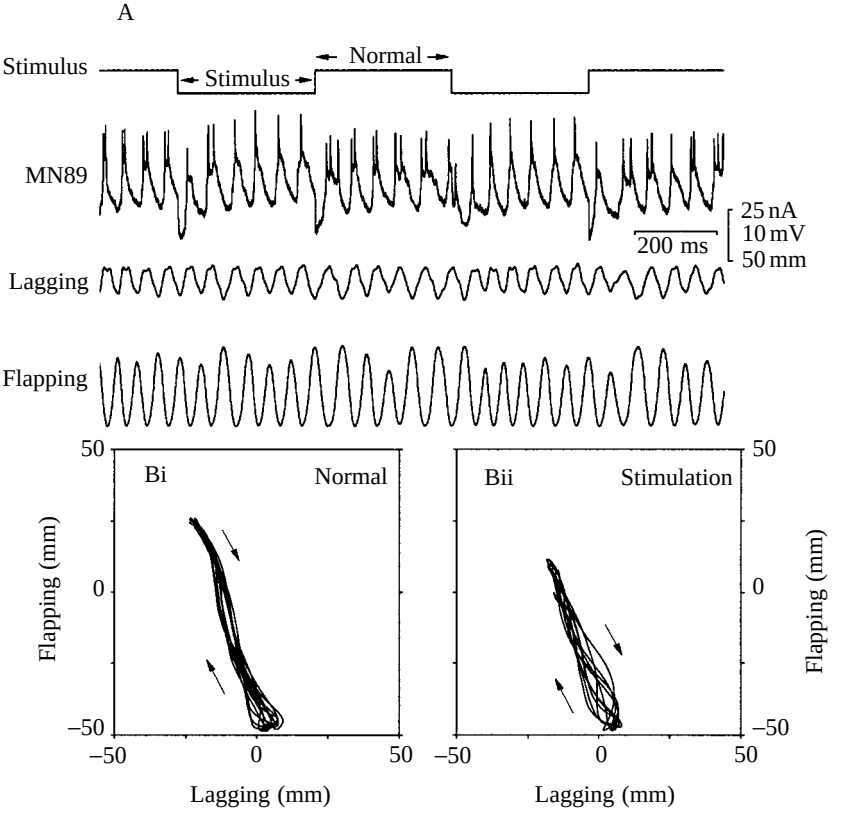

Fig. 8. (A) Effects of stimulation of elevator MN89 on wing movements. Hyperpolarizing current injection into the motoneurone resulted in a decrease in its spike activity and led to a decrease in the amplitude of the upward movement of the wing. (B) Wingtip path during normal flight cycles (Bi, left) and during flight cycles with MN98 inhibition (Bii, right). Six wingtip paths were superimposed. The arrows indicate the direction of wing movement.

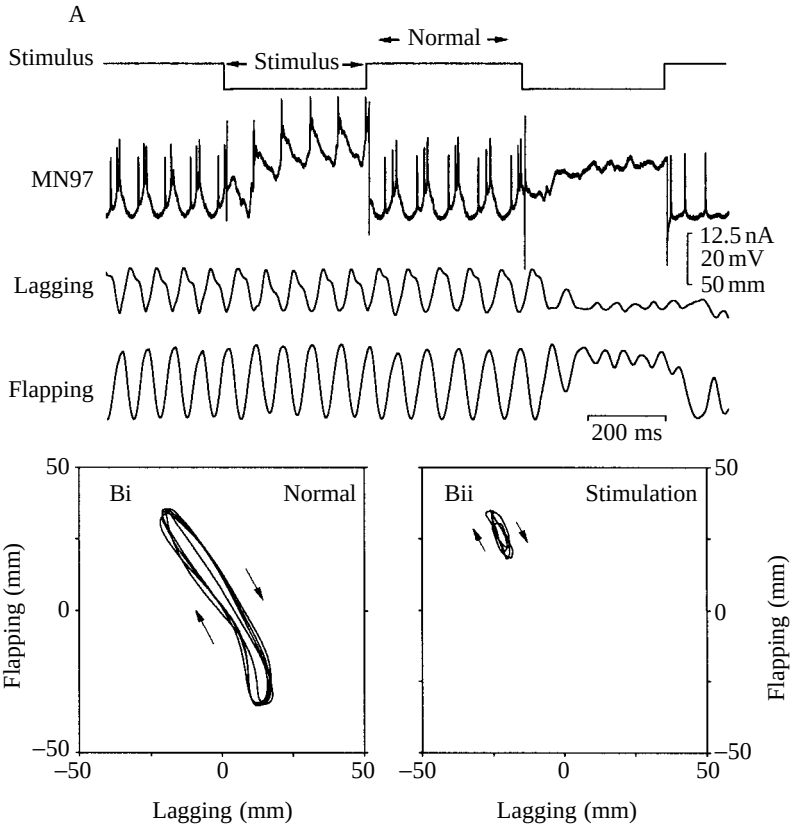

Fig. 9. (A) Effects of inhibition of depressor motoneurone MN97 on wing movements. Hyperpolarizing current injection into the motoneurone resulted in a decrease in its spike activity to one spike per cycle (left), resulting in only minor effects on the wing movement. A complete block of spike activity (right) caused a decrease in the amplitude of the downward movement followed by a cessation of flight activity. (B) Wingtip path during normal flight cycles (Bi, left) and during wing movements with complete MN97 inhibition (Bii, right). Four wingtip paths were superimposed. The arrows indicate the direction of wing movement.

reduction in the amplitude of the upward movement, which was only 33 mm during MN97 stimulation (Fig. 10B). Since the end of the downstroke remained the same as in normal flight sequences, the total amplitude of the flapping movement was approximately half of the undisturbed movement. The total amplitude of the lagging movement was slightly increased from 49 mm to 52 mm (Fig. 10B). These changes resulted in the wingtip path having a flat oval shape tilted backwards with respect to the normal pattern (Fig. 10B). Similar results were obtained when motoneurone MN98 (second basalar) was stimulated in the same way.

In addition to these effects on wing movement, depolarization of MN97 also had an effect on flight frequency. Flight frequency was 14.2 Hz when the motoneurone was not stimulated, but decreased to 12.5 Hz during phases of enhanced MN97 activity (Fig. 10A). Thus, in this case, the increased motoneurone activity affected both the generation of the movement pattern and the flight rhythm.

Discussion

Methods for measurement of wing movements

Several methods have been used to analyse the wing movements of flying locusts in two dimensions: stroboscopic filming techniques (Weis-Fogh, 1956; Wilson and Weis-Fogh, 1962; Wolf, 1990), high-speed cameras (Weis-Fogh, 1956; Baker, 1979; Robertson and Reye, 1992; Zarnack, 1972), inductive measurement of wing movements (Koch, 1977; Zarnack, 1978, 1988; Schwenne and Zarnack, 1987; Waldmann and Zarnack, 1988) and the optoelectronic technique used in the present study (Hedwig and Becher, 1995). An advantage of stroboscopic or high-speed film recordings is that they can be used for very small insects (Nachtigall, 1966). However, the temporal resolution of the technique is limited, and usually only short flight sequences can be recorded. The inductive technique allows simultaneous measurement of the movement components of all four wings. However, owing to its data processor, the temporal resolution of that technique was limited and movement data could be sampled at intervals of 2 ms only.

Compared with these techniques, the new optoelectronic method provides a very high temporal resolution. The wing coordinates are sampled at intervals of 100 μs, giving 20 times as many data points per wingbeat cycle as the inductive technique. Thus, even at the end of the wing strokes, the wingtip path can be resolved clearly. A major advantage of this method is that it can easily be combined with intracellular electrophysiological recordings. Although it is limited at present to measuring the flapping and lagging movement components of a single wing only, it may be expanded in future to include the movements of all four wings. This would allow investigations into intersegmental coordination. Measurements of pronation and supination of the wing would be possible if two light guides were used, attached to the anterior and posterior edges of a wing.

Movements of the forewing tip

Data on the path of the forewing tip during the tethered flight

of locusts are available from photographic studies (Jensen, 1956; Zarnack, 1972) and from inductive recordings (Schwenne and Zarnack, 1987; Zarnack, 1988; Waldmann and Zarnack, 1988; Wortmann and Zarnack, 1993). In all these studies, locusts were flown in an upright position in the laminar airflow of a wind tunnel. Data obtained during steady flight show an oval drop-shaped wingtip path (see Fig. III.3 in Jensen, 1956; Fig. 5 in Zarnack, 1972). However, measurements obtained during the performance of specific flight manoeuvres revealed the variability of the wing movement, which can follow different oval or figure-of-eight-shaped patterns (Figs 3, 9 in Zarnack, 1988; Fig. 12 in Waldmann and Zarnack, 1988; Figs 2, 4 in Wortmann and Zarnack, 1993).

Our experiments required that the locusts had to be flown upside down, and there is evidence that this flight position results in changes in the motor pattern (Stevenson and Kutsch, 1987). The locusts were also not flown in a laminar airstream. However, the path of the wingtip we obtained under these conditions was very similar to the patterns described in earlier studies. The oval drop-shaped wingtip path, which was the most common pattern we observed, indicates stable, steady flight performance (Fig. 3A). In some cases, the locusts produced different patterns (Fig. 3B,C), some being similar to patterns recorded during yaw manoeuvres (Zarnack, 1988). Since open-loop conditions during tethered flight increase the variability of the motor pattern (Möhl, 1985, 1988; Thüring, 1986; Schmidt and Zarnack, 1987), the variation in wingtip movements we recorded may not be surprising. A certain level of variability of flight performance may have to be accepted in experiments in which kinematic measurements and intracellular recordings are carried out simultaneously. However, in such experiments, the quality of flight performance is always clearly indicated by the pattern of wing movements.

Correspondence between motoneurone activity and wingtip movement

The temporal relationship between the muscle activity and wing movements of tethered flying locusts was analysed by Wilson and Weis-Fogh (1962) using stroboscopic photographs triggered by the activity in the electromyograms (EMGs) of flight muscles. These recordings showed that elevator activity occurs at the end of the downstroke and that the direct depressors are active before or just after the end of the upstroke. Simultaneous recordings of wing movement and flight muscle EMGs have shown the periods within the wingtip path when the flight muscles are active (Zarnack, 1988; Waldmann and Zarnack, 1988; Reuse, 1991). The scatter diagrams in Fig. 12 of Waldmann and Zarnack (1988) indicate that the elevator M84 is active just before the end of the downstroke and that for depressor M97 there is an elongated scatter of activity during the upward movement of the wing. These scatter diagrams are very similar to those obtained for M83 and M97 in the present study (Fig. 4).

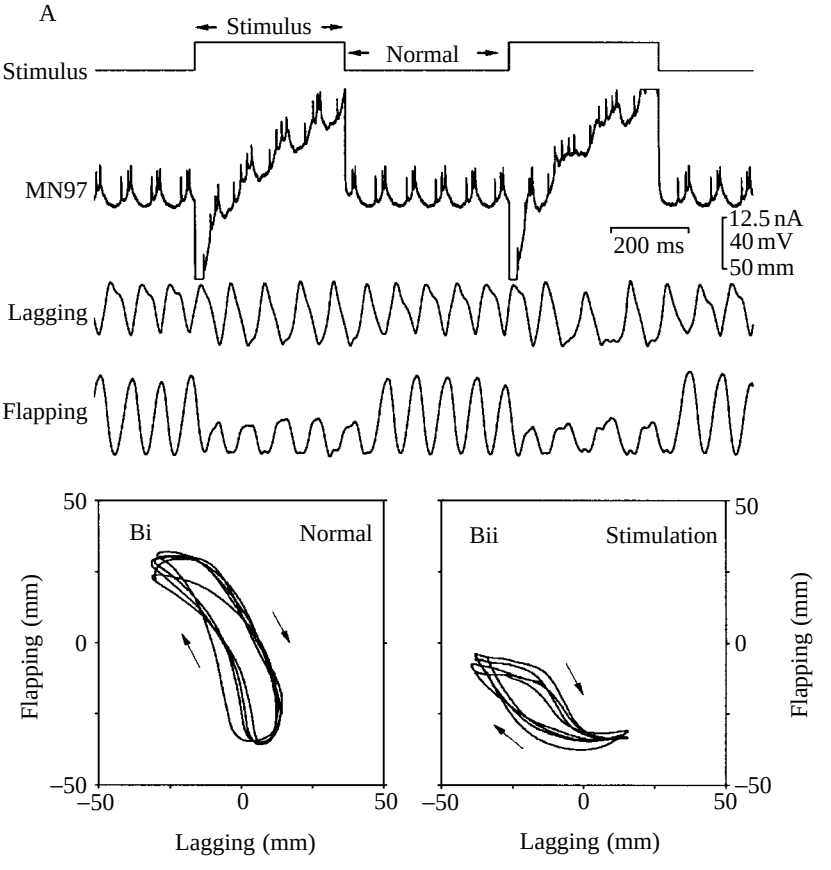

Fig. 10. (A) Effects of stimulation of depressor motoneurone MN97 on wing movements. Depolarization the motoneurone resulted in an increase in its spike activity and led to a decrease in the amplitude of the upward movement of the wingtip. (B) Wingtip path during normal flight sequences (Bi, left) and during flight cycles with MN97 stimulation (Bii, right). Four wingtip paths were superimposed. The arrows indicate the direction of wing movement.

Two-dimensional measurements of wing movements in combination with intracellular recordings from flight motoneurones have not been obtained previously. Our data indicate increased variability of the motor pattern during intracellular recordings compared with locusts in which EMGs only are recorded. The positions of the wingtip path when the muscles M83 and M97 were active (Fig. 4) exhibit much less scatter than in the corresponding diagrams for the action potentials of motoneurones MN83 and MN97 (Figs 5, 6). The scatter and phase diagrams demonstrate that, during intracellular recordings, the motoneurones may be more active and may start their spike activity much earlier in the wingbeat cycle than when only electromyographic recordings are made. This may indicate that the dissection required for intracellular recordings might induce considerable variability in flight performance. The variability encountered in our experiments, however, was not high enough to impede analysis of the effects of motoneurone activity on wing movement.

Effects of motoneurone stimulation

The interactions among motor activity, wing movements and aerodynamic forces are of major interests in furthering the understanding of locust flight. Various attempts have been made to analyse the functional roles of individual muscles in flight control. One convincing way of studying this problem is to modulate the activity patterns of known muscles while simultaneously recording the wing movements. This experimental approach ensures that changes observed in the movements are actually caused by the experimentally manipulated muscle activity. Using this approach, Zarnack (1982) used extracellular stimulation of the first basalar muscle (M97) to analyse its contribution to the generation of wing movements, and Wolf (1990) demonstrated the functional significance of a steering muscle (M85) in the control of wing rotation. However, extracellular stimulation can only increase the activity of muscles; it cannot reduce their activity. Thus, to date, there are only limited data available on the relationship between elevator or depressor motoneurone activity and wing movements. The lack of knowledge is even greater regarding the activity of flight interneurones.

The data obtained here by using stimulation of motoneurones clearly demonstrate the effects of single muscles or even single motor units on the performance of wing movements. The amplitude of the flapping movement of the wing clearly decreased when the activity of elevator motoneurones (MN83 and MN89) was reduced. The movement amplitude decreased when the number of spikes per wingbeat cycle in MN83 and MN89 decreased from two to one; however, the effects were strongest when M83 activity was completely suppressed. The present data provide no evidence for the effects on wing movement of increasing elevator activity to three or four spikes per wingbeat cycle. This verifies the force measurements on locust flight muscles of Mizisin and Josephson (1987). They demonstrated a 20 % increase in the power output of the muscles during double activation compared with single activation. However, there was no further increase in the power output when the muscles were activated by bursts of 3–5 stimuli. In the present study, intracellular stimulation induced simultaneous changes in the burst length and the phase of muscle activity. Therefore, we cannot yet separate these effects, which have been discussed previously as parameters for flight control (Möhl and Zarnack, 1977; Baker, 1979; Thüring, 1986; Zarnack, 1988; Waldmann and Zarnack, 1988). On the basis of their almost identical membrane potential oscillations and the very similar synaptic drive they receive from the central pattern generator (Hedwig and Pearson, 1984; Wolf and Pearson, 1987*b*), elevator motoneurones are regarded as a very homogeneous group. However, the elevator muscles are of different sizes and they therefore differ in the amount of power they supply to the wing movement. Functional differences in the activity of individual muscles in the generation of the wing movement are therefore likely and, indeed, are indicated by the elevator stimulation experiments, in which MN83 inhibition had a greater effect than MN89 inhibition (compare Figs 7, 8) and there was no effect when the activity of MN90 was altered. Thus, although elevator motoneurones may receive a similar synaptic drive, they may have to be thought of as being more differentiated in functional terms.

Zarnack and Möhl (1977), Möhl and Zarnack (1977) and Baker (1979) obtained recordings from different depressor muscles. They analysed the activity patterns during steering behaviour and correlated changes in the temporal pattern of motor activity with the steering behaviour. However, simultaneous recordings of the movements were not obtained. Causal relationships between time shifts in muscle activity or changes in burst length and changes in wing movements could therefore not be established. Simultaneous recordings of muscle activity and wing movements were carried out by Zarnack (1988) and Waldmann and Zarnack (1988) with the intention of analysing the role of the direct depressor muscles on wing rotations and flapping movements. The correlations between movement parameters and muscle (M97, M99) activity revealed their synergistic role in forewing pronation. They found that the downstroke movement was greatly reduced in the absence of M97 depressor activity (see also Koch, 1977). Stimulation of depressor muscle M97 demonstrated distinct effects on the simultaneously recorded wing movements (Zarnack, 1982).

In the present experiments, we did not observe differences in the wing movement corresponding to whether motoneurone MN97 was active with one or three spikes per wingbeat cycle (Fig. 9). However, increasing the motoneurone activity to five spikes had a significant effect on the movement (Fig. 10). This increased activity of MN97 did not increase the amplitude of downstroke movement but, since it occurred early in the wingbeat cycle, it was almost in phase with the elevator activity. Therefore, it caused a distinct decrease in the amplitude of the upstroke. This result is in agreement with data in Zarnack (1982, Figs 23–26) showing that M97 stimulation was most effective in reducing the upstroke when it occurred in phase with elevator activity. Thus, in the case of muscle

M97, the phase of muscle activity may be regarded as an important parameter in the control of the wing movement (Zarnack, 1988).

Complete inhibition of MN97 spike activity led to a reduction in the amplitude of the downstroke, followed by a cessation of flight activity. The changes in flight frequency caused by MN97 stimulation are surprising and may be explained by the importance of sensory feedback in the flight system. It is well established that sensory feedback from the passive movements of a single wing can modulate flight frequency (Wendler, 1974), and tegula stimulation seems to be essential for the generation of elevator activity (Wolf and Pearson, 1988). Altered wing movements due to motoneurone stimulation will inevitably also lead to changes in sensory feedback. As a consequence, it is conceivable that MN97 inhibition indirectly led to a reduction in sensory feedback, which resulted in the observed decrease in wingbeat frequency. Our data therefore emphasize the functional significance of the first basalar muscle M97 in the generation of wing movements and the performance of flight behaviour.

Future prospects

The simultaneous recording of wing movements and motoneurone stimulation has provided insight into the functional significance of motoneurone activity in the generation of wing movements that was not revealed using earlier techniques. It emphazises the specific roles of individual motoneurones in the generation of wing movements which, in particular cases, may be as important as the role of sensory feedback (Wolf and Pearson, 1988). In future, this approach could reveal the functional significance of identified flight interneurones (Robertson and Pearson, 1983, 1984) in the control of wing movements.

We thank Professor N. Elsner for supporting this project and Professor W. Zarnack for valuable comments on the manuscript. Mitsubishi Rayon Co. generously provided a sample of the optical fibre CK-4, a basic prerequisite for these experiments. Several companies kindly provided samples of optical fibres (Schott, Cunz, Polytec, Optocom, Reinshagen). Melles Griot and Newport helped to select a suitable laser and to design the optical equipment. We are also most grateful to M. Glahe, H. Badstübner and W. Stieler for the development of the electronic circuit.

References

BAKER, P. S. (1979). The wing movements of flying locusts during steering behaviour. *J. comp. Physiol.* A **131**, 49–58.

HEDWIG, B. AND BECHER, G. (1995). Flügelbewegungen und intrazelluläre Ableitungen von Flugneuronen an stationär fliegenden Wanderheuschrecken. *Vh. dt. zool. Ges*. **88**, 85.

HEDWIG, B. AND KNEPPER, M. (1992). NEUROLAB, a comprehensive program for the analysis of neurophysiological and behavioural data. *J. Neurosci. Meth.* **45**, 135–148.

HEDWIG, B. AND PEARSON, K. G. (1984). Patterns of synaptic input to identified flight motoneurons in the locust. *J. comp. Physiol* A **154**, 745–760.

JENSEN, M. (1956). Biology and physics of locust flight. III. The aerodynamics of locust flight. *Phil. Trans. R. Soc. B* **239**, 511–552.

KNEPPER, M. AND HEDWIG, B. (1996). NEUROLAB, a PC-program for the processing of neurobiological data. *Comp. Meth. Prog. Biomed*. **52**, 75–77.

KOCH, U. T. (1977). A miniature movement detector applied to recording of wingbeat in *Locusta*. *Fortschr. Zool*. **24**, 327–332.

MIZISIN, A. P. AND JOSEPHSON, R. K. (1987). Mechanical power output of locust flight muscle. *J. comp. Physiol.* A **160**, 413–419.

MÖHL, B. (1985). The role of proprioception in locust flight control. I. Asymmetry and coupling within the time pattern of motor units. *J. comp. Physiol.* A **156**, 93–101.

MÖHL, B. (1988). Short-term learning during flight control in *Locusta migratoria*. *J. comp. Physiol*. A **163**, 803–812.

MÖHL, B. AND ZARNACK, W. (1977). Activity of the direct downstroke flight muscles of *Locusta migratoria* (L.) during steering behaviour in flight. II. Dynamics of the time shift and changes in the burst length. *J. comp. Physiol.* A **18**, 235–247.

NACHTIGALL, W. (1966). Die Kinematik der Schlagflügelbewegungen von Dipteren. Methodische und analytische Grundlagen zur Biophysik des Insektenflugs. *Z. vergl. Physiol.* **52**, 155–211.

REUSE, G. (1991). Analyse neuromuskulärer und kinematischer Steuergrößen im Flugsystem der Wüstenheuschrecke (*Schistocerca gregaria*). Dissertation, Universität Göttingen. 123pp.

ROBERTSON, R. M. AND PEARSON, K. G. (1983). Interneurons in the flight system of the locust: distribution, connections and resetting properties. *J. comp. Neurol.* **215**, 33–50.

ROBERTSON, R. M. AND PEARSON, K. G. (1984). Interneuronal organisation in the flight system of the locust. *J. Insect Physiol.* **30**, 95–101.

ROBERTSON, R. M. AND REYE, D. N. (1992). Wing movements associated with collision-avoidance manoeuvres during flight in the locust *Locusta migratoria*. *J. exp. Biol.* **63**, 231–258.

SCHMIDT, J. AND ZARNACK, W. (1987). The motor pattern of locusts during visually induced rolling in long-term flight. *Biol. Cybernetics* **56**, 397–410.

SCHWENNE, T. AND ZARNACK, W. (1987). Movements of the hindwings of *Locusta migratoria*, measured with miniature coils. *J. comp. Physiol.* A **160**, 657–666.

STEVENSON, P. A. AND KUTSCH, W. (1987). A reconsideration of the central pattern generator concept for locust flight. *J. comp. Physiol.* A **161**, 115–129.

STEWART, W. (1978). Functional connections between cells as revealed by dye-coupling with a highly fluorescent naphthalmine tracer. *Cell* **14**, 741–759.

THÜRING, D. A. (1986). Variability of motor output during flight steering in locusts. *J. comp. Physiol.* A **158**, 653–664.

USHERWOOD, P. AND GRUNDFEST, H. (1965). Peripheral inhibition in skeletal muscle of insects. *J. Neurophysiol.* **28**, 497–518.

WALDMANN, B. AND ZARNACK, W. (1988). Forewing movements and motor activity during roll manoeuvers in flying desert locusts. *Biol. Cybernetics* **59**, 325–335.

WEIS-FOGH, T. (1956). Biology and physics of locust flight. II. Flight performance of the desert locust (*Schistocerca gregaria*). *Phil. Trans. R. Soc. B* **239**, 459–510.

WEIS-FOGH, T. AND JENSEN, M. (1956). Biology and physics of locust flight. I. Basic principles in insect flight. *Phil. Trans. R. Soc. B* **239**, 416–458.

WENDLER, G. (1974). The influence of proprioreceptive feedback on locust flight co-ordination. *J. comp. Physiol.* **88**, 173–200.

WILSON, D. M. AND WEIS-FOGH, T. (1962). Patterned activity of co-ordinated motor units, studied in flying locusts. *J. exp. Biol.* **39**, 643–667.

WOLF, H. (1990). On the function of a locust flight steering muscle and its inhibitory innervation. *J. exp. Biol.* **150**, 55–80.

WOLF, H. (1993). The locust tegula: significance for flight rhythm generation, wing movement control and aerodynamic force production. *J. exp. Biol.* **182**, 229–253.

WOLF, H. AND PEARSON, K. G. (1987*a*). Intracellular recordings from interneurons and motoneurons in intact flying locusts. *J. Neurosci. Meth.* **21**, 345–354.

WOLF, H. AND PEARSON, K. G. (1987*b*). Comparison of motor patterns in the intact and deafferented flight system of the locust. II. Intracellular recordings from flight motoneurons. *J. comp. Physiol.* A **160**, 269–279.

WOLF, H. AND PEARSON, K. G. (1988). Proprioceptive input patterns elevator activity in the locust flight system. *J. Neurophysiol.* **59**, 1831–1853.

WORTMANN, M. (1991). Rolldrehmoment, Auftrieb und Vortrieb in Abhängigkeit von einer Vielzahl aerodynamischer relevanter Parameter der Flügelbewegungen der Wüstenheuschrecke. Dissertation, Universität Göttingen. 146pp.

WORTMANN, M. AND ZARNACK, W. (1993). Wing movements and lift regulations in the flight of desert locusts. *J. exp. Biol.* **182**, 57–69.

ZARNACK, W. (1972). Flugbiophysik der Wanderheuschrecke (*Locusta migratoria* L.). I. Die Bewegungen der Vorderflügel. *J. comp. Physiol.* A **78**, 356–395.

ZARNACK, W. (1978). A transducer recording continuously 3-dimensional rotations of biological objects. *J. comp. Physiol.* A **126**, 161–168.

ZARNACK, W. (1982). Kinematische, aerodynamische und neurophysiologisch-funktions-morphologische Untersuchungen des Heuschreckenflugs. Habilitationsschrift, Universität Göttingen.

ZARNACK, W. (1988). The effect of forewing depressor activity on wing movement during locust flight. *Biol. Cybernetics* **59**, 55–70.

ZARNACK, W. AND MÖHL, B. (1977). Activity of direct downstroke flight muscles of *Locusta migratoria* (L.) during steering behaviour in flight. I. Patterns of time shift. *J. comp. Physiol.* A **118**, 215–233.